Applied and Environmental Microbiology, Mar. 2009, p. 1703–1716 Vol. 75, No. 6
0099-2240/09/$08.00+0 doi:10.1128/AEM.02081-08

Reconfiguring the Quorum-Sensing Regulator SdiA of *Escherichia coli* To Control Biofilm Formation via Indole and *N*-Acylhomoserine Lactones▽†

Jintae Lee,[1] Toshinari Maeda,[1] Seok Hoon Hong,[1] and Thomas K. Wood[1,2,3]*

Artie McFerrin Department of Chemical Engineering,[1] Department of Biology,[2] and Zachry Department of Civil Engineering,[3] 220 Jack E. Brown Building, Texas A&M University, College Station, Texas 77843-3122

Received 8 September 2008/Accepted 10 January 2009

SdiA is a homolog of quorum-sensing regulators that detects *N*-acylhomoserine lactone (AHL) signals from other bacteria. *Escherichia coli* uses SdiA to reduce its biofilm formation in the presence of both AHLs and its own signal indole. Here we reconfigured SdiA (240 amino acids) to control biofilm formation using protein engineering. Four SdiA variants were obtained with altered biofilm formation, including truncation variants SdiA1E11 (F7L, F59L, Y70C, M94K, and K153X) and SdiA14C3 (W9R, P49T, N87T, frameshift at N96, and L123X), which reduced biofilm formation by 5- to 20-fold compared to wild-type SdiA in the presence of endogenous indole. Whole-transcriptome profiling revealed that wild-type SdiA reduced biofilm formation by repressing genes related to indole synthesis and curli synthesis compared to when no SdiA was expressed, while variant SdiA1E11 induced genes related to indole synthesis in comparison to wild-type SdiA. These results suggested altered indole metabolism, and corroborating the DNA microarray results in regard to indole synthesis, variant SdiA1E11 produced ninefold more indole, which led to reduced swimming motility and cell density. Also, wild-type SdiA decreased curli production and *tnaA* transcription, while SdiA1E11 increased *tnaA* transcription (*tnaA* encodes tryptophanase, which forms indole) compared to wild-type SdiA. Hence, wild-type SdiA decreased biofilm formation by reducing curli production and motility, and SdiA1E11 reduced biofilm formation via indole. Furthermore, an AHL-sensitive variant (SdiA2D10, having four mutations at E31G, Y42F, R116H, and L165Q) increased biofilm formation sevenfold in the presence of *N*-octanoyl-DL-homoserine lactone and *N*-(3-oxododecatanoyl)-L-homoserine lactone. Therefore, SdiA can be evolved to increase or decrease biofilm formation, and biofilm formation may be controlled by altering sensors rather than signals.

It is important to be able to control biofilms containing multiple species for engineering applications. For example, in the first engineered biofilm (a microbial consortium), we engineered a *Bacillus subtilis* biofilm to secrete the peptide antimicrobials indolicidin and bactenecin to inhibit the growth of sulfate-reducing bacteria in the biofilm (without harming the protective *B. subtilis* biofilm) and thereby to decrease corrosion (25). We also developed the first synthetic signaling circuit to control biofilm formation and used it to control the biofilm formation of *Escherichia coli* and *Pseudomonas fluorescens* by manipulating the extracellular concentration of the signal indole (32).

To increase the tool kit for manipulating biofilm formation, we investigated here how SdiA of *E. coli* controls biofilm formation and whether this protein may be evolved to control biofilm formation through the use of extracellular signals. We chose SdiA as a tool because SdiA interacts with one of the extracellular signals produced by *E. coli*, indole (32, 34), as well as recognizes acylhomoserine lactones (AHLs) from other bacteria (35) and binds with them (62).

SdiA of *E. coli*, named for its ability to *s*uppress cell *d*ivision *i*nhibitors (54), is a 240-amino-acid protein that belongs to the LuxR family of transcriptional regulators (23) that induces the *ftsQAZ* locus involved in cell division (54); however, its role in *E. coli* cell physiology remains enigmatic (35). Using SdiA, *Salmonella enterica* and *E. coli* detect the quorum-sensing signal AHLs produced by other bacteria, although they do not synthesize AHLs (35); AHLs control social behavior like biofilm formation (16) and virulence (57). Also, SdiA is stabilized upon binding of AHLs (62) and consists of an autoinducer-binding domain (residues 1 to 171) (63) and a helix-turn-helix DNA binding domain (residues 197 to 216) (54).

SdiA represses the expression of virulence factors by interacting with unknown stationary-phase signals in *E. coli* O157:H7 (27), enhances multidrug resistance by stimulating multidrug efflux pumps in *E. coli* (43), and increases the acid tolerance of *E. coli* upon exposure to AHLs (52). We found that SdiA decreases early *E. coli* biofilm formation 51-fold (32), enhances acid resistance (32), and is required to reduce *E. coli* biofilm formation in the presence of AHLs as well as in the presence of the stationary-phase signal indole (32, 34). Indole is an *E. coli* quorum-sensing signal (31) that works primarily at temperatures found outside the human host (34) and reduces biofilm formation (4, 17, 31, 32, 34). Therefore, SdiA, via direct or indirect interaction with indole and AHLs,

* Corresponding author. Mailing address: Texas A&M University, Chemical Engineering, 220 Jack E. Brown Building, College Station, TX 77843-3122. Phone: (979) 862-1588. Fax: (979) 865-6446. E-mail: Thomas.Wood@chemail.tamu.edu.

† Supplemental material for this article may be found at http://aem.asm.org/.

▽ Published ahead of print on 23 January 2009.

TABLE 1. Strains and plasmids used

Strain or plasmid	Genotype/relevant characteristics[a]	Source or reference
Strains		
E. coli K-12 BW25113	*lacI*^{q} *rrnB*$_{T14}$ Δ*lacZ*$_{WJ16}$ *hsdR514* Δ*araBA-D*$_{AH33}$ Δ*rhaBAD*$_{LD78}$	3
E. coli K-12 BW25113 *sdiA*	K-12 BW25113 Δ*sdiA* Ω Km^{r}	3
E. coli K-12 BW25113 *tnaA*	K-12 BW25113 Δ*tnaA* Ω Km^{r}	3
E. coli K-12 BW25113 *mtr*	K-12 BW25113 Δ*mtr* Ω Km^{r}	3
E. coli K-12 BW25113 *csgB*	K-12 BW25113 Δ*csgB* Ω Km^{r}	3
E. coli K-12 BW25113 *csgE*	K-12 BW25113 Δ*csgE* Ω Km^{r}	3
E. coli K-12 BW25113 *csgF*	K-12 BW25113 Δ*csgF* Ω Km^{r}	3
E. coli K-12 BW25113 *adrA*	K-12 BW25113 Δ*adrA* Ω Km^{r}	3
E. coli K-12 BW25113 *tnaA sdiA*	K-12 BW25113 Δ*tnaA* Δ*sdiA* Ω Km^{r}	This study
E. coli K-12 BW25113 *mtr sdiA*	K-12 BW25113 Δ*mtr* Δ*sdiA* Ω Km^{r}	This study
Plasmids		
pCA24N	Empty vector; Cm^{r}	28
pCA24N-*sdiA*	pCA24N *pT5-lac*::*sdiA*; expresses SdiA derived from *E. coli*	28
pCA24N-*adrA*	pCA24N *pT5-lac*::*adrA*; expresses AdrA derived from *E. coli*	28
pCP20	Ap^{r} and Cm^{r} plasmid with temperature-sensitive replication and thermal induction of FLP synthesis	10

[a] Km^{r}, Cm^{r}, and Ap^{r} stand for kanamycin, chloramphenicol, and ampicillin resistance, respectively.

is a key protein for intraspecies and interspecies cell communication as well as for biofilm formation.

Directed evolution has been utilized to show the evolutionary pliability of the AHL response regulator LuxR of *Vibrio fischeri* by broadening its substrate range (13), by increasing its sensitivity to octanoyl-L-homoserine lactone (13), and by eliminating its response to 3-oxohexanoyl-homoserine lactone with a carbonyl substituent at the third carbon (14). A site-directed mutagenesis of the LuxR-type quorum-sensing activator TraR of *Agrobacterium tumefaciens* has been performed on the residues forming hydrogen bonds with *N*-oxooctanoyl-L-homoserine lactone to alter AHL specificity (9) and to alter AHL binding (37). Also, spontaneous mutations of LasR (another LuxR family member from *Pseudomonas aeruginosa*), including a truncation mutant, cause phenotypic diversification, such as differences in colony morphology, pyocyanin and elastase production, swarming motility, and cell viability in the late stationary phase (36).

Since cell communication and biofilm formation are important for bacterial survival in microbial consortia (26), bacteria may readily evolve response regulators for enhanced fitness. We investigated here how the quorum-sensing regulator SdiA influences biofilm formation and then hypothesized that SdiA may be evolved for enhanced or reduced biofilm formation in the absence or presence of cell signals such as indole and AHLs. Both indole (53) and AHLs (20) are extracellular signals, so they were chosen as potential signals for reconfiguring SdiA to respond to them. Using random mutagenesis (error-prone PCR [epPCR]), SdiA libraries were obtained and screened for altered biofilm formation in the presence and absence of indole and two AHLs, *N*-butyryl-DL-homoserine lactone (C4-DL-HSL), and *N*-(3-oxooctanoyl)-L-homoserine lactone (3o-C8-L-HSL). After obtaining four biofilm mutants, DNA microarrays were utilized to understand the mechanism of biofilm reduction by wild-type SdiA and by the evolved SdiA variant SdiA1E11 that was 20-fold more effective at reducing biofilm formation. In addition, site-directed mutagenesis, saturation mutagenesis, double mutations, and real-time, reverse transcription-PCR (RT-PCR) were used to investigate the mechanism by which SdiA1E11 controls biofilm; the primary mechanism is its influence on the concentration of indole. Hence, our goals were to discern how wild-type SdiA functions in biofilms, to control biofilm formation by evolving SdiA, and to determine how the SdiA variants function.

MATERIALS AND METHODS

Bacterial strains and materials. The strains utilized are shown in Table 1. *E. coli* K-12 BW25113 and its isogenic mutants were obtained from the National Institute of Genetics in Japan (Keio collection) (3); the *sdiA* deletion in BW25113 was confirmed by DNA microarrays (34). BW25113 *sdiA* was used as the host for screening plasmids containing *sdiA* alleles created via epPCR; these alleles were expressed using pCA24N-*sdiA* (28). The empty pCA24N plasmid does not express the green fluorescent protein (28), and all the SdiA variants are not green fluorescent protein fusions. All *E. coli* strains were initially streaked from −80°C glycerol stocks on Luria-Bertani (LB) agar plates (48) containing 50 μg/ml kanamycin (for the host) and 30 μg/ml chloramphenicol (for maintaining pCA24N-*sdiA*). All experiments were performed at 30°C since SdiA (52) and indole (34) are primarily active at this temperature in *E. coli*. SdiA was expressed using 1 mM isopropyl-β-D-thiogalactopyranoside (IPTG; Sigma, St. Louis, MO).

For cell density measurements, BW25113 *sdiA* harboring various SdiA variants was grown in LB agar (25 ml) containing IPTG in 250-ml flasks at 250 rpm, and the optical density was measured at 600 nm. Each experiment was performed with at least four independent cultures. The specific growth rates of each strain were determined by measuring the cell turbidity at 600 nm of two independent cultures as a function of time using turbidity values less than 0.7.

Indole was purchased from Fisher Scientific Co. (Pittsburgh, PA). C4-DL-HSL, *N*-hexanoyl-DL-homoserine lactone (C6-DL-HSL), *N*-octanoyl-DL-homoserine lactone (C8-DL-HSL), *N*-decanoyl-DL-homoserine lactone (C10-DL-HSL), *N*-dodecanoyl-DL-homoserine lactone (C12-DL-HSL), 3o-C8-L-HSL, and *N*-(3-oxotetradecanoyl)-L-homoserine lactone (3o-C14-L-HSL) were purchased from Sigma. *N*-butyryl-L-homoserine lactone (C4-L-HSL) and *N*-(3-oxododecanoyl)-L-homoserine lactone (3o-C12-L-HSL) were purchased from Cayman Chemical (Ann Arbor, MI). C4-DL-HSL, C4-L-HSL, C6-DL-HSL, and C8-DL-HSL were dissolved in water. Indole, 3o-C8-L-HSL, C10-DL-HSL, C12-DL-HSL, 3o-C12-L-HSL, and 3o-C14-L-HSL were dissolved in dimethylformamide (DMF). DMF alone or water alone was used as a control.

epPCR, saturation mutagenesis, and truncation of SdiA. *sdiA* from plasmid pCA24N-*sdiA* under the control of the *pT5-lac* promoter was mutated by epPCR as described previously (19) using two primers, SdiA front and SdiA reverse (Table 2). The epPCR product was cloned into pCA24N-*sdiA* using BseRI and PstI after treating the plasmid with Antarctic phosphatase (New England Bio-

TABLE 2. Primers used for epPCR, DNA sequencing, RT-PCR, and confirmation of the double mutants

Purpose	Primer	Sequence
epPCR of SdiA	SdiA front	5′-AGGCGTATCACGAGGCCCTTTC-3′
	SdiA reverse	5′-CAGTCACGATGAATTCCCCTAG-3′
DNA sequencing	Seq primer 1	5′-CACCGATCGCCCTTCCCAACAGTTGC-3′
	Seq primer 2	5′-GCAGTTACTGGTGCGCGAAAG-3′
RT-PCR for *tnaA* and housekeeping gene *rrsG*	TnaA front	5′-TGAAGAAGTTGGTCCGAATAACGTG-3′
	TnaA reverse	5′-CTTTGTATTCTGCTTCACGCTGCTT-3′
	RrsG front	5′-TATTGCACAATGGGCGCAAG-3′
	RrsG reverse	5′-ACTTAACAAACCGCCTGCGT-3′
Confirmation of the *sdiA* mutation	SdiA up	5′-AATGCGATGGCTTGCAAAAGTAATT-3′
	SdiA down	5′-AGCAAATTAAACAAGCCTACCGTCA-3′
Confirmation of the *tnaA* mutation	TnaA up	5′-CTGGCGAATTAATCGGTATAGCAGA-3′
	TnaA down	5′-GATCAGTCATGATGCCACCTTTAGA-3′
Confirmation of the *mtr* mutation	Mtr up	5′-GTACTCGTGTACTGGTACAGTGCAA-3′
	Mtr down	5′-TCCTACATAGACCTGATAAGCGAAG-3′

labs, Beverly, MA). The ligation mixture was electroporated into BW25113 *sdiA* as described previously (19).

To perform saturation mutagenesis and to truncate the carboxyl terminus of SdiA, site-directed mutagenesis was performed using the QuikChange XL site-directed mutagenesis kit (Stratagene, La Jolla, CA). DNA primers (see Table S1 in the supplemental material) were designed to substitute all possible amino acids at M94 and W95 for SdiA1E11 as a parent protein and at H28, E29, I30, E31, Y39, D40, Y41, and Y42 for SdiA2D10 as a parent protein. Also, DNA primers (see Table S1 in the supplemental material) were designed to introduce a stop codon at wild-type SdiA codons R16, Q33, T53, A73, L93, A110, and L133. The resulting *sdiA* nucleotide sequences were confirmed by DNA sequencing using the ABI Prism BigDye Terminator cycle sequencing ready kit (PerkinElmer, Wellesley, MA).

Biofilm screening of SdiA variants. Biofilm mutants were screened using polystyrene 96-well microtiter plates and an adapted crystal violet assay (41). The crystal violet dye stains both the air-liquid interface and bottom liquid-solid interface biofilm, and the total biofilm formation at both interfaces was measured at 540 nm, whereas cell growth was measured at 620 nm. BW25113 *sdiA* colonies expressing SdiA variants from pCA24N-*sdiA* were grown overnight in 96-well plates with 200 μl of LB medium at 250 rpm, the overnight cultures were diluted (1:100) in 300 μl of LB medium containing IPTG, and the biofilm was formed for 24 h without shaking (where appropriate, 500 μM indole, 10 μM C4-DL-HSL, or 10 μM 3o-C8-L-HSL was also added). Total biofilm formation was normalized by cell growth (turbidity at 620 nm) to avoid overestimating changes due to growth effects. As controls, BW25113 *sdiA* with empty pCA24N and pCA24N-*sdiA* (wild-type *sdiA*) were used. Interesting biofilm mutants were reanalyzed by restreaking the colonies on fresh LB plates and by performing another biofilm assay. *sdiA* mutant alleles were sequenced with two primers, Seq primer 1 and Seq primer 2 (Table 2). Each data point was averaged from more than 12 replicate wells (6 wells from two independent cultures). Protein truncations of variants SdiA1E11, SdiA14C3, and SdiA16G12 were verified using standard Laemmli discontinuous sodium dodecyl sulfate-polyacrylamide gel electrophoresis (48).

Indole assay. Extracellular and intracellular concentrations of indole were measured with reverse-phase high-performance liquid chromatography as described previously (32). BW25113 *sdiA* harboring various *sdiA* plasmids was grown in LB medium containing IPTG to a turbidity of 3.0 at 600 nm. The turbidity of 3.0 represents a time point when wild-type *E. coli* secretes approximately 300 μM indole. Each experiment was performed with two independent cultures.

Swimming motility and curli assays. Swimming motility was measured as described previously (32). Exponentially grown cells (turbidity of 1.0 at 600 nm) were used to assay motility in plates containing 1% (wt/vol) tryptone, 0.25% (wt/vol) NaCl, and 0.3% (wt/vol) agar. In order to test the effect of indole on motility, indole was added to the agar plate. The motility halos were measured after 20 h in the presence of IPTG. Each experiment was performed with two replicates from two independent cultures.

For curli, LB agar medium containing 20 μg/ml Congo red (Sigma), 10 μg/ml Coomassie brilliant blue (Sigma), 15 g/liter agar, and IPTG was used as described previously to visualize *E. coli* curli expression after a 28-h incubation at 30°C (44). Since Congo red binds both curli and cellulose (15), a cellulose-specific assay using calcofluor (15) was used to determine if curli or cellulose was identified by the Congo red assay. For the cellulose assay, BW25113 *adrA* was used as a negative cellulose control and BW25113 *adrA*/pCA24N-*adrA* was used as a positive cellulose control.

Total RNA isolation for DNA microarrays. BW25113 *sdiA*/pCA24N, BW25113 *sdiA*/pCA24N-*sdiA*, and BW25113 *sdiA*/pCA24N-*sdiA1E11* were grown in 250 ml LB medium containing IPTG for 12 h with 10 g of glass wool (Corning Glass Works, Corning, NY) in 1-liter Erlenmeyer shake flasks to form a robust biofilm (45). RNA was isolated from the biofilm cells as described previously using sonication and a bead beater (45).

DNA microarray analysis. The *E. coli* GeneChip Genome 2.0 array contains 10,208 probe sets for open reading frames, rRNA, tRNA, and intergenic regions for four *E. coli* strains: MG1655, CFT073, O157:H7-Sakai, and O157:H7-EDL933. cDNA synthesis, fragmentation, and hybridizations were as described previously (22). Hybridization was performed for 16 h, and the total cell intensity was scaled to an average value of 500. The background values, noise values, and scaling factors of the three arrays were examined and were comparable. The intensities of the polyadenosine RNA controls were used to monitor the labeling process. For each binary microarray comparison of differential gene expression, if the gene with the higher transcription rate did not have a consistent transcription rate based on the 11 probe pairs (*P* value of less than 0.05), these genes were discarded. A gene was considered differentially expressed when the *P* value for comparing two chips was lower than 0.05 (to ensure that the change in gene expression was statistically significant and that false positives arise less than 5%) and when the expression ratio was higher (fourfold) than the standard deviation for all K-12 genes of the microarrays (2.1-fold for SdiA versus when no SdiA was expressed and 2.6-fold for SdiA1E11 versus SdiA) (46). Gene functions were obtained from the Affymetrix-NetAffx Analysis Center (http://www.affymetrix.com/analysis/index.affx).

Double mutations. BW25113 *tnaA sdiA* and BW25113 *mtr sdiA* were constructed as described previously using the rapid gene knockout procedure with P1 transduction (38) by using plasmid pCP20 (12) to eliminate the kanamycin resistance (Km^r) gene. The four mutations of the two double mutants were confirmed by PCR with six primers (Table 2), SdiA up, SdiA down, TnaA up, TnaA down, Mtr up, and Mtr down, which flank each gene of interest and confirm both the insertion and elimination of the Km^r gene.

RT-PCR. To corroborate the DNA microarray data, the transcription of *tnaA* was quantified with primers TnaA front and TnaA reverse (Table 2) using RT-PCR (4). BW25113 *sdiA* harboring pCA24N (no *sdiA* control), pCA24N-*sdiA*, or pCA24N-*sdiA1E11* was grown in LB medium containing IPTG to a turbidity of 1.8 at 600 nm when *E. coli* produces indole. The RNA was isolated from the suspension cells as described previously (45). Housekeeping gene *rrsG* (16S rRNA) with primers RrsG front and RrsG reverse (Table 2) was used to normalize the expression data. A total of 36 RT-PCRs with two independent cultures were performed based on three RT-PCRs for *tnaA* and the *rrsG* housekeeping gene for the three different samples (BW25113 *sdiA*/pCA24N, pCA24N-*sdiA*, and pCA24N-*sdiA1E11*) using an iCycler (Bio-Rad, Hercules, CA) and MyiQ software (Bio-Rad).

Protein modeling. The amino acid sequences of the SdiA1E11 (residues 1 to 152) were modeled into the known three-dimensional structure of the *E. coli* SdiA (residues 1 to 171; Protein Data Bank accession code 2avx) (62). The three-dimensional model was obtained using the SWISS-MODEL server (http://swissmodel.expasy.org/) (49). The molecular visualization program PyMOL (http://pymol.sourceforge.net/) was utilized to make the protein image of the molecular model.

Microarray data accession number. The microarray data summarized in Table 3 have been deposited in the NCBI Gene Expression Omnibus (18) (http://www.ncbi.nlm.nih.gov/geo/) and are accessible through accession number GSE11779.

TABLE 3. Partial list of the most differentially expressed genes for biofilm cells of BW25113 *sdiA* strains expressing SdiA, no SdiA, and SdiA1E11[a]

Functional group and/or gene	b no.[b]	Change in expression (fold)		Description and/or function[c]
		SdiA vs no SdiA	SdiA1E11 vs SdiA	
Indole-related				
sdiA	b1916	5,043.0	−2.3	LuxR/UhpA family, regulation of cell division *ftsQAZ* genes, sensing AHLs, required for indole signaling
tnaC	b3707	−22.6	16.0	Tryptophanase leader peptide
tnaA	b3708	−7.5	6.5	Tryptophanase
tnaB	b3709	−16.0	9.8	Low-affinity tryptophan permease
Fimbria and curli				
sfmH	b0533	−2.3	4.6	Fimbrial assembly protein
csgG	b1037	−21.1	3.2	Curli production assembly/transport component
csgF	b1038	−36.8	4.3	Curli production assembly/transport component
csgE	b1039	−24.3	3.7	Curli production assembly/transport component, second curli operon
csgD	b1040	−17.1	3.0	Two-component transcriptional regulator for second curli operon, family of LuxR/UhpA
csgB	b1041	−29.9	2.8	Minor curlin subunit precursor
csgA	b1042	−17.1	2.6	Curlin major subunit, coiled surface structures, cryptic
csgC	b1043	−10.6	3.2	Putative curli production protein
yfcV	b2339	−2.0	4.0	Putative fimbria-like protein
AI-2 uptake				
lsrA	b1513	−7.0	3.0	AI-2 uptake
lsrC	b1514	−4.9	3.0	AI-2 uptake
lsrD	b1515	−5.3	3.5	AI-2 uptake
lsrB	b1516	−13.9	3.2	AI-2 uptake
lsrF	b1517	−9.8	4.0	Function unknown, involved in AI-2 catabolism
lsrG	b1518	−7.5	3.0	Function unknown, involved in AI-2 catabolism
Acid resistance				
ariR	b1166	−4.9	3.7	AriR, regulator of acid resistance influenced by indole
ymgC	b1167	−4.0	3.7	Hypothetical protein in AriR operon
gadC	b1492	−14.9	3.0	Glutamic acid decarboxylase
gadB	b1493	−32.0	3.5	Glutamate decarboxylase isozyme
gadX	b3516	−5.7	2.5	Putative AraC-type regulatory protein
gadA	b3517	−21.1	3.5	Glutamate decarboxylase A, isozyme, PLP dependent
hdeB	b3509	−19.7	3.2	Acid resistance protein HdeB
hdeA	b3510	−14.9	3.2	10K-L protein, periplasmic protein related to acid resistance protein
hdeD	b3511	−11.3	2.6	Acid resistance protein HdeD
Cold shock and stress				
cspH	b0989	8.0	−4.0	Cold shock protein CspH
cspG	b0990	4.9	−3.5	Cold shock protein CspG
cspI	b1552	2.8	−4.0	Cold shock protein CspI
cspB	b1557	5.3	−4.0	Cold shock protein CspB
cspF	b1558	10.6	−4.9	Cold shock protein CspF
rtT	b1228	8.0	−4.6	*rtT* RNA, may modulate the stringent response
katE	b1732	−5.7	2.1	Catalase HPII
csiE	b2535	−7.0	4.0	Stationary-phase inducible protein
csiD	b2659	−14.9	3.7	Carbon starvation-induced (*csi*) gene
uspB	b3494	−6.5	2.3	Universal stress protein B
ibpB	b3686	4.0	1.1	16-kDa heat shock protein B
ibpA	b3687	5.3	−1.6	16-kDa heat shock protein A
oxyS	b4458	4.9	−4.0	Global regulatory RNA OxyS
Metabolism and transport				
psiF	b0384	−7.5	2.5	Phosphate starvation-inducible protein *psiF* precursor
queA	b0405	4.3	−2.6	*S*-Adenosylmethionine:tRNA ribosyltransferase-isomerase
poxB	b0871	−6.1	1.6	Pyruvate dehydrogenase/oxidase, FAD and thiamine PPi binding
agp	b1002	−6.1	4.9	Acid glucose-1-phosphatase
potB	b1125	4.0	−2.5	Spermidine/putrescine transport system permease protein
potA	b1126	4.6	−2.5	Spermidine/putrescine transport ATP-binding protein
narY	b1467	−6.1	3.2	Cryptic nitrate reductase 2 β subunit
narZ	b1468	−8.0	4.3	Cryptic nitrate reductase 2 α subunit

Continued on following page

TABLE 3—*Continued*

Functional group and/or gene	b no.[b]	Change in expression (fold)		Description and/or function[c]
		SdiA vs no SdiA	SdiA1E11 vs SdiA	
narU	b1469	−5.3	3.2	Nitrite extrusion protein 2
osmC	b1482	−6.1	1.9	Osmotically inducible protein C
osmE	b1739	−8.0	2.1	Osmotically inducible lipoprotein E precursor
rnfB	b1628	4.0	−2.5	Electron transport complex protein
astE	b1744	−8.6	4.6	Succinylglutamate desuccinylase
astB	b1745	−12.1	4.3	Succinylarginine dihydrolase
astD	b1746	−8.0	4.0	Succinylglutamic semialdehyde dehydrogenase
astA	b1747	−13.9	4.6	Arginine succinyltransferase
cstC	b1748	−12.1	4.9	Succinylornithine transaminase
flu	b2000	−1.4	7.0	Antigen 43 (Ag43) phase-variable biofilm formation autotransporter
fbaB	b2097	−8.6	2.8	Fructose-bisphosphate aldolase class I
yojH	b2210	5.7	−2.6	Malate:quinone oxidoreductase
tktB	b2465	−6.5	1.7	Transketolase 2
gabD	b2661	−13.0	2.6	Succinate-semialdehyde dehydrogenase [$NADP^+$]
gabT	b2662	−13.0	3.5	4-Aminobutyrate aminotransferase
gabP	b2663	−8.6	3.5	GABA permease
hycB	b2724	−3.5	4.6	Formate hydrogenlyase subunit 2
hyuA	b2873	−2.6	4.0	Phenylhydantoinase
ravA	b3012	−5.3	2.3	2,5-Diketo-d-gluconic acid reductase A
glgS	b3049	−7.0	2.5	Glycogen synthesis protein
secG	b3175	4.0	−2.6	Protein export membrane protein
rpsI	b3230	4.6	−2.6	30S ribosomal protein S9
rpsQ	b3311	4.6	−2.6	30S ribosomal protein S17
glpD	b3426	5.7	−4.9	sn-Glycerol-3-phosphate dehydrogenase (aerobic)
ggt	b3447	−6.5	2.6	γ-Glutamyltranspeptidase
ugpB	b3453	−5.7	2.1	Glycerol-3-phosphate-binding periplasmic protein precursor
ddpX	b1488	−7.5	3.0	d-Ala-d-Ala dipeptidase, Zn dependent
dppF	b3540	−8.0	3.5	Dipeptide transport ATP-binding protein
dppD	b3541	−8.0	3.5	Dipeptide transport ATP-binding protein
dppC	b3542	−8.6	4.0	Dipeptide transport system permease protein
aldB	b3588	−12.1	4.0	Aldehyde dehydrogenase B (lactaldehyde dehydrogenase)
rnpA	b3704	4.3	−3.0	RNase P protein component
bglF	b3722	4.3	2.6	Glucoside PTS transporter
qor	b4051	−6.5	1.9	Quinone oxidoreductase
actP	b4067	−17.1	5.3	Acetate permease
acs	b4069	−10.6	4.6	Acetyl-coenzyme A synthetase
melA	b4119	−6.1	2.6	α-Galactosidase
blc	b4149	−6.1	2.1	Outer-membrane lipoprotein *blc* precursor
aidB	b4187	−6.1	2.0	AidB protein
ytfQ	b4227	−6.1	2.1	Putative d-ribose transport protein (ABC superfamily)
treA	b1197	−7.5	2.8	Periplasmic trehalase precursor
treC	b4239	4.3	−3.0	Trehalose-6-phosphate hydrolase
treB	b4240	4.3	−3.0	PTS system, trehalose-specific IIBC component
Other				
rhlE	b0797	6.5	−3.7	Putative ATP-dependent RNA helicase
rmf	b0953	9.8	2.6	Hypothetical protein
sfa	b0991	4.9	−3.5	Sfa protein
wrbA	b1004	−16.0	3.2	Flavoprotein WrbA
ftsT	b1569	−2.3	4.0	Transcriptional repressor of cell division inhibition protein
hisL	b2018	2.3	−9.8	His operon leader peptide
fis	b3261	4.3	−2.3	DNA-binding protein Fis gene
slp	b3506	−14.9	1.9	Outer-membrane protein slp precursor
spf	b3864	4.9	−3.7	Spot 42 RNA
phnB	b4107	−9.8	2.8	PhnB protein
mutL	b4170	−1.3	−4.3	MutHLS complex, enzyme in methyl-directed mismatch repair
isrB	b4434	6.1	−6.1	Intergenic sequence sRNA
isrC	b4435	−1.3	4.0	Intergenic sequence sRNA
micF	b4439	−7.0	2.1	Regulatory antisense RNA affecting *ompF* expression
Hypothetical				
yahK	b0325	−5.7	2.6	Hypothetical zinc-type alcohol dehydrogenase-like protein
yahO	b0329	−7.0	2.8	Hypothetical protein
ybaS	b0485	−7.5	2.3	Probable glutaminase YbaS

Continued on following page

TABLE 3—*Continued*

Functional group and/or gene	b no.[b]	Change in expression (fold)		Description and/or function[c]
		SdiA vs no SdiA	SdiA1E11 vs SdiA	
ybaT	b0486	−6.5	2.5	Hypothetical transport protein
ybcL	b0545	−5.3	2.6	DLP12 prophage
ybgA	b0707	−5.3	2.3	Hypothetical protein
ybgS	b0753	−9.2	2.8	Hypothetical protein
ybhB	b0773	−5.3	2.1	Hypothetical protein
ybiY	b0824	−2.5	4.3	Putative pyruvate formate-lyase 3 activating enzyme gene
ybjP	b0865	−7.0	1.7	Putative lipoprotein
ycaC	b0897	−9.8	4.9	Hypothetical protein
ycgB	b1188	−9.8	2.8	Hypothetical protein
ychH	b1205	−6.5	2.5	Hypothetical protein
yciD	b1256	−9.8	2.5	Hypothetical protein
yciL	b1269	4.0	−2.8	Hypothetical protein
ydfK	b1375	6.1	−4.0	Hypothetical protein
ynaF	b1376	−5.7	1.7	Hypothetical protein
ydbC	b1406	−5.7	3.0	Hypothetical protein
ydcJ	b1423	−8.6	4.0	Hypothetical protein
ydcS	b1440	−13.9	4.6	Putative ABC transporter periplasmic-binding protein gene
ydcT	b1441	−11.3	5.7	Putative ABC transporter ATP-binding protein
ydcU	b1442	−7.5	3.2	Hypothetical ABC transporter permease protein
ydcV	b1443	−8.0	3.7	Hypothetical ABC transporter
ydcW	b1444	−12.1	5.7	Putative betaine aldehyde dehydrogenase
yddJ	b1470	−2.6	4.6	Hypothetical protein
yddS	b1487	−6.1	3.0	Putative ABC transport system periplasmic binding protein
ydeI	b1536	−5.7	3.5	Hypothetical protein
ydgN	b1629	4.6	−2.6	Electron transport complex protein
ydiM	b1690	−3.2	4.3	Putative transport protein (MFS family)
ydjN	b1729	4.6	−2.1	Hypothetical symporter
yeaH	b1784	−8.6	2.8	Hypothetical protein
yedP	b1955	−5.3	2.3	Hypothetical protein
yedU	b1967	−8.6	2.5	Hypothetical protein
yeeF	b2014	5.7	−2.1	Hypothetical protein
yegP	b2080	−6.5	2.3	Hypothetical protein
yehE	b2112	−6.1	1.6	Hypothetical protein
yohC	b2135	−5.7	2.8	Hypothetical protein
yeiN	b2165	−3.0	4.3	Hypothetical protein
ygaF	b2660	−9.8	2.6	Hypothetical protein
ygaQ	b2654	−2.6	4.0	Hypothetical protein
ygaR	b2655	−2.3	4.0	Hypothetical protein
yqaD	b2658	−2.3	4.0	Hypothetical protein
ygaM	b2672	−7.5	2.1	Hypothetical protein
ygdI	b2809	−6.1	1.7	Hypothetical protein
ygeL	b2856	−1.4	4.0	Predicted DNA-binding transcriptional regulator
ygeN	b2857	−2.1	4.0	Hypothetical protein
yqjE	b3099	−5.7	−1.5	Hypothetical protein
yhbC	b3170	3.5	−4.0	Hypothetical protein
yhbE	b3184	4.6	−3.5	Hypothetical protein
yhdG	b3260	4.3	−2.5	Hypothetical protein
yhiE	b3512	−12.1	2.8	Hypothetical protein
yjcH	b4068	−24.3	5.7	Hypothetical protein
yjdI	b4126	−6.5	1.5	Hypothetical protein
yjdJ	b4127	−5.3	2.0	Hypothetical protein

[a] Strains BW25113 *sdiA*/pCA24N-*sdiA* (expressing SdiA), BW25113 *sdiA*/pCA24N (expressing no SdiA), and BW25113 *sdiA*/pCA24N-*sdiA1E11* (expressing SdiA1E11) were grown in LB medium with 30 μg/ml chloramphenicol and 1 mM IPTG for 12 h at 30°C. Raw data for the two DNA microarrays are available using GEO series accession number GSE11779. Primarily, genes differentially expressed above fourfold are shown, although some related genes are shown for completeness.

[b] Blattner number.

[c] PLP, pyridoxal phosphate; FAD, flavin adenine dinucleotide; GABA, gamma-aminobutyric acid; PTS, phosphotransferase system; IIBC, PTS permease II domains B and C; sRNA, noncoding small RNA; MFS, major facilitator superfamily.

RESULTS

Random mutagenesis of SdiA and biofilm screening. To reconfigure SdiA for greater control of biofilm formation with and without external signals, epPCR mutagenesis using both manganese and an unbalanced deoxynucleoside triphosphate mixture (19) was used to mutate randomly *sdiA*. The epPCR products were cloned into plasmid pCA24N-*sdiA*, and the plasmids were transformed into *E. coli* K-12 BW25113 *sdiA* so that there was no background SdiA in these cells, and all the

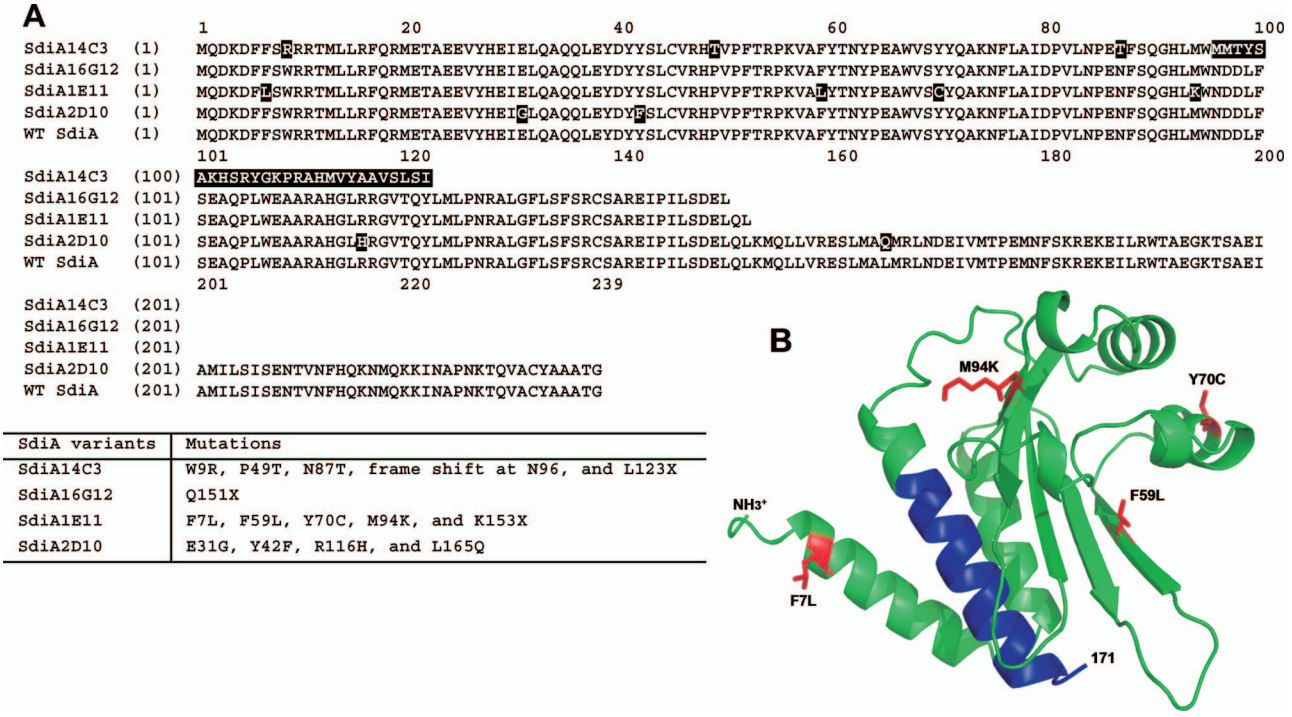

SdiA variants	Mutations
SdiA14C3	W9R, P49T, N87T, frame shift at N96, and L123X
SdiA16G12	Q151X
SdiA1E11	F7L, F59L, Y70C, M94K, and K153X
SdiA2D10	E31G, Y42F, R116H, and L165Q

FIG. 1. (A) Protein sequences of the SdiA epPCR variants. Amino acid changes are indicated by the black highlight. SdiA14C3 has a frameshift at N96 due to the deletion of one base pair. (B) Modeled protein structure of SdiA1E11. Truncated region (residues 153 to 171) is shown as a blue ribbon, and the mutations (F7L, F59L, Y70C, and M94K) are shown in red. WT indicates wild type.

changes in phenotype were due to plasmid-encoded SdiA variants. By sequencing five random colonies, the maximum error rate was determined to be 0.94%. Colonies (4,577) were screened for altered biofilm formation with and without extracellular signals (500 μM indole, 10 μM C4-DL-HSL, or 10 μM 3o-C8-L-HSL), which resulted in the identification of four biofilm variants (Fig. 1A). The mutations of SdiA1E11, SdiA14C3, and SdiA16G12 decreased biofilm formation at 24 h in the absence of extracellular signals (Fig. 2B). The SdiA2D10 variant increased biofilm formation in the presence of 3o-C8-L-HSL in LB medium. Biofilm screening with C4-DL-HSL and indole did not lead to an interesting variant.

Unexpectedly, SdiA1E11, SdiA14C3, and SdiA16G12 (Fig. 1A) had truncations in SdiA so that they lack the carboxyl DNA-binding domain (residues 196 to 216) (54) (Fig. 1A). SdiA1E11 has five mutations at F7L, F59L, Y70C, M94K, and K153X (X indicates termination); SdiA14C3 has mutations at W9R, P49T, N87T, the frameshift at N96, and L123X; and SdiA16G12 has mutation Q151X. Also, the AHL-sensitive SdiA2D10 variant has four mutations at E31G, Y42F, R116H, and L165Q (Fig. 1A). In order to eliminate any possible chromosomal mutation effects, all the pCA24N-*sdiA* plasmids identified during the first and second screens were retransformed into BW25113 *sdiA*, and the changes in biofilm formation were confirmed; hence, the changes in biofilm formation are due to the changes in the *sdiA* gene on the plasmid.

SdiA variants decrease *E. coli* biofilm formation. Previously, we discovered that the deletion of *sdiA* causes a 51-fold increase in biofilm formation in LB medium at 30°C after 8 h (32); hence, SdiA reduces biofilm formation. Consistently, deleting *sdiA* resulted in an 18-fold increase in biofilm formation in LB medium after 8 h (Fig. 2A). As expected, overexpressing wild-type SdiA from pCA24N-*sdiA* reduced biofilm formation 3.5-fold after 8 h compared to when no SdiA was expressed (empty vector pCA24N) (Fig. 2A). Similar results were observed in LB glucose (LB glu) medium after 8 h (Fig. 2A); hence, the biofilm phenotype due to SdiA could be partially complemented (full complementation probably was not achieved because of expression differences due to the nonnative promoter and differences in copy number).

Biofilm formation in the presence of the SdiA variants was compared at both 8 h and 24 h since the differences in biofilm formation upon deleting wild-type *sdiA* gradually decrease with time (32) (Fig. 2A and B). Two truncation variants, SdiA1E11 and SdiA16G12, lacking the carboxy-terminal DNA-binding domain of SdiA resulted in a significant reduction of biofilm formation (5- to 10-fold) in both LB and LB glu media after 8 h (Fig. 2A). After 24 h, SdiA1E11 further decreased biofilm formation 5- to 20-fold in both LB and LB glu media, SdiA14C3 decreased biofilm formation 4- to 6-fold in both LB and LB glu media, and SdiA16G12 decreased biofilm formation 8-fold primarily in LB glu medium (Fig. 2B). Inhibition of biofilm formation via the evolved SdiA variants was more significant in LB glu medium probably because of the catabolite repression of *tnaA* (5) which should reduce indole concentrations for wild-type SdiA. These results show that the quorum-sensing regulator SdiA may be evolved to alter dramatically *E. coli* biofilm and may be altered to keep biofilm formation low for long periods.

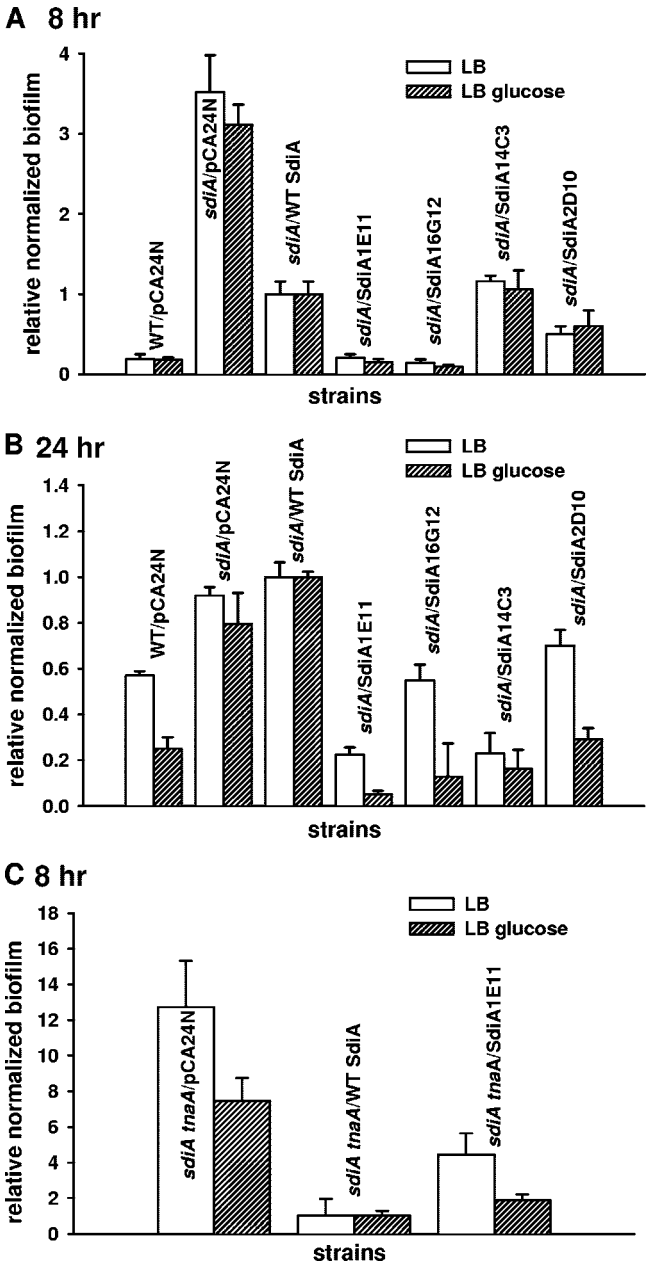

FIG. 2. Relative biofilm formation in the presence of endogenous indole and normalized by bacterial growth (turbidity at 620 nm) for BW25113 *sdiA* cells expressing the SdiA variants in LB and LB glu media after 8 h (A) and after 24 h (B) (raw data are shown in Table S2A and S2B in the supplemental material) and relative biofilm formation normalized by bacterial growth (turbidity at 620 nm) for BW25113 *sdiA tnaA* cells expressing wild-type SdiA and SdiA1E11 after 8 h (C) at 30°C. No extracellular signal was added. Normalized biofilm data are relative to BW25113 *sdiA*/pCA24N-*sdiA* (A and B) and BW25113 *sdiA tnaA*/pCA24N-*sdiA* (C). Each data point is the average of the results from at least 12 replicate wells from two independent cultures, and one standard deviation is shown. SdiA was expressed using 1 mM IPTG.

The modeled protein structure of SdiA1E11 is shown in Fig. 1B and is based on the known structure of *E. coli* SdiA (residues 1 to 171, the autoinducer-binding domain) (62). The K153X truncation of SdiA1E11 causes it to lose most of the long α5 alpha helix (residues 148 to 168, shown as a blue ribbon in Fig. 1B).

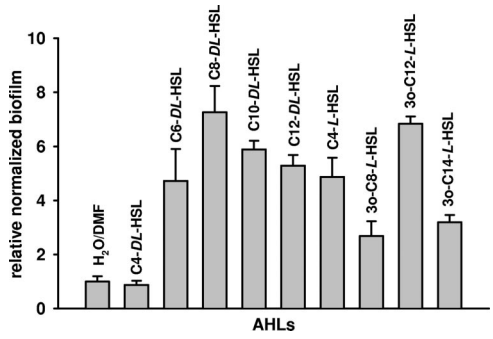

FIG. 3. Relative biofilm formation in LB glu medium after 24 h at 30°C for BW25113 *sdiA* cells expressing SdiA2D10 in the presence of added AHLs and with endogenous indole. Biofilm formation was normalized by bacterial growth (turbidity at 620 nm) and is relative to cells without added AHLs. C4-DL-HSL, C4-L-HSL, C6-DL-HSL, and C8-DL-HSL were dissolved in water, and C10-DL-HSL, C12-DL-HSL, 3o-C8-L-HSL, 3o-C12-L-HSL, and 3o-C14-L-HSL were dissolved in DMF. AHLs were added at the beginning of culturing. Raw data are shown in Table S3 in the supplemental material. Each data point is the average of the results from at least 12 replicate wells from two independent cultures, and one standard deviation is shown. SdiA2D10 was expressed using 1 mM IPTG.

Reconfiguring SdiA to alter biofilm formation with AHLs. Previously we reported that the addition of exogenous AHLs (10 μM of *N*-butyryl-, *N*-hexanoyl-, and *N*-octanoyl-DL-homoserine lactones) inhibited *E. coli* biofilm formation up to 27% without inhibiting growth (32). Also, *N*-hexanoyl-L-homoserine lactone significantly decreases *E. coli* biofilm in mixed culture with *Serratia plymuthica* (40). Here, the SdiA2D10 variant was identified, and the mutations of SdiA2D10 increased biofilm formation 1.9-fold in the presence of 10 μM 3o-C8-L-HSL in LB medium (normalized biofilm, 0.69 ± 0.02 versus 1.31 ± 0.05) while 3o-C8-L-HSL addition to wild-type SdiA reduced biofilm formation by 6% under these conditions (normalized biofilm, 1.00 ± 0.06 versus 0.94 ± 0.02) in LB medium after 24 h; hence, the four mutations of SdiA2D10 reversed the impact of this AHL on biofilm formation. Both biofilm variants SdiA1E11 and SdiA14C3 did not change biofilm formation upon adding 10 μM 3o-C8-L-HSL (normalized biofilm, 0.22 ± 0.03 versus 0.26 ± 0.03 for SdiA1E11 and 0.23 ± 0.09 versus 0.25 ± 0.09 for SdiA14C3) in LB medium after 24 h.

Moreover, the AHL-sensitive SdiA2D10 and wild-type SdiA were tested with nine different *N*-acylhomoserine lactones with 4 to 14 carbons for the variable side chain at 10 μM in LB and LB glu media. The mutations of SdiA2D10 increased biofilm formation (four- to sevenfold) in the presence of six AHLs (C4-L-HSL, C6-DL-HSL, C8-DL-HSL, 3o-C8-L-HSL, C10-DL-HSL, C12-DL-HSL, and 3o-C12-L-HSL) in LB glu medium after 24 h (Fig. 3), while the wild-type SdiA decreased biofilm formation less than 1.3-fold with the same AHLs compared to when no AHLs were present (data not shown). Also, these AHLs increased biofilm formation maximally twofold with SdiA2D10 in LB medium (data not shown). Hence, AHLs enhanced biofilm formation via the evolved SdiA2D10 primarily in LB glu medium in which indole production is reduced due to the catabolite repression of *tnaA* (5). The results show

SdiA may be altered to enhance biofilm formation of *E. coli* in the presence of AHLs produced from other bacteria.

Whole-transcriptome analysis of SdiA and SdiA1E11 in biofilm cells. To understand how the overexpression of SdiA regulates gene expression in biofilm cells, DNA microarrays were used to determine differential gene expression for biofilm cells with the overexpression of SdiA versus biofilm cells without SdiA (empty plasmid) in LB medium for 12 h. It was found that 208 genes were regulated significantly (more than fourfold) with SdiA than without SdiA; 37 genes were induced and 171 genes were repressed (Table 3). Most notable was that two indole-related genes (*tnaAB*) and the *tna* leader region (*tnaC*) were highly repressed (7.5- to 23-fold) upon overexpressing SdiA. Hence, indole-related genes are repressed by wild-type SdiA. Also, genes were repressed related to curli synthesis (*csgDEFG* and *csgBAC*), the autoinducer-2 (AI-2) uptake operon (*lsrACDBFG*), acid resistance (*gadA*, *gadBC*, *gadX*, *hdeAB*, and *hdeD*), and a newly found acid resistance regulator *ariR* (33), while five cold shock protein genes (*cspH*, *cspG*, *cspI*, *cspB*, and *cspF*) were induced in biofilm cells with SdiA (Table 3). These results indicate that SdiA influences the regulation of many genes including genes related to cell communication. However, the transcriptional level of the cell division regulator of *ftsQAZ* and the AI-2 synthesis gene of *luxS* were not changed by the overexpression of SdiA.

Another whole-transcriptome study was used to determine differential gene expression for biofilm cells with the overexpression of the SdiA1E11 variant (the most important biofilm mutant) versus biofilm cells with the overexpression of wild-type SdiA grown in LB for 12 h. It was found that 60 genes were regulated more significantly (more than fourfold) with SdiA1E11 than with wild-type SdiA; 46 genes were induced and 14 genes were repressed (Table 3). In contrast to the comparison of the results when wild-type SdiA was expressed and when no SdiA was expressed, most notable was that two indole-related genes (*tnaAB*) and the *tna* leader region (*tnaC*) were highly induced (6.5- to 16-fold) upon overexpressing SdiA1E11. Hence, indole genes are preferentially induced with SdiA1E11. Also, genes related to curli synthesis, acid resistance (*gadA*, *gadBC*, *hdeB*, and *ariR*), and the AI-2 uptake operon (*lsrKRACDBFG*) were induced in biofilm cells with SdiA1E11, while five cold shock protein genes (*cspH*, *cspG*, *cspI*, *cspB*, and *cspF*) were repressed (Table 3). The results indicate that the evolved SdiA1E11 differentially regulates gene expression from wild-type SdiA.

RT-PCR. RT-PCR was used to corroborate the whole-transcriptome results for wild-type SdiA and SdiA1E11. As expected, the overexpression of wild-type SdiA repressed *tnaA* transcription by 48-fold ($\Delta\Delta C_T = 5.6 \pm 2.5$, where C_T is the threshold cycle of the target genes) compared to when no SdiA was expressed, which is consistent with the previous report (55). In contrast, the overexpression of SdiA1E11 induced (226-fold; $\Delta\Delta C_T = 7.8 \pm 2.3$) *tnaA* transcription compared to the overexpression of wild-type SdiA; hence, the mutations that lead to SdiA1E11 alter the regulation of *tnaA* by SdiA.

Wild-type SdiA decreases curli production. Since curli fibers are required for both adhesion and biofilm formation (42) and the overexpression of SdiA most repressed (11- to 37-fold) curli genes (*csgDEFG* and *csgBAC*) (Table 3), curli production was measured upon overexpressing SdiA and SidA1E11 using a Congo red plate assay. SdiA decreased dramatically curli production, while SdiA1E11 decreased curli production to a small extent (Fig. 4A); these data corroborate well the microarray data (Table 3). Since Congo red binds both curli and cellulose (15), and CsgD controls the production of curli as well as cellulose (15), a cellulose specific assay using calcofluor was also used to investigate cellulose production upon the expression of SdiA. Unlike curli production in colonies, cellulose production with planktonic cells increased slightly upon overexpressing both SdiA (1.3 ± 0.1-fold) and SdiA1E11 (1.8 ± 0.3-fold) compared to when no SdiA was expressed. These results suggest that the reduction of Congo red binding is due to a decrease in curli production (Fig. 4A). Moreover, three curli mutants (*csgB*, *csgE*, and *csgF*) formed two- to threefold less biofilm than the wild-type strain (Fig. 4B) as expected. The results suggest that wild-type SdiA inhibits curli production, which partially explains the decrease in biofilm formation.

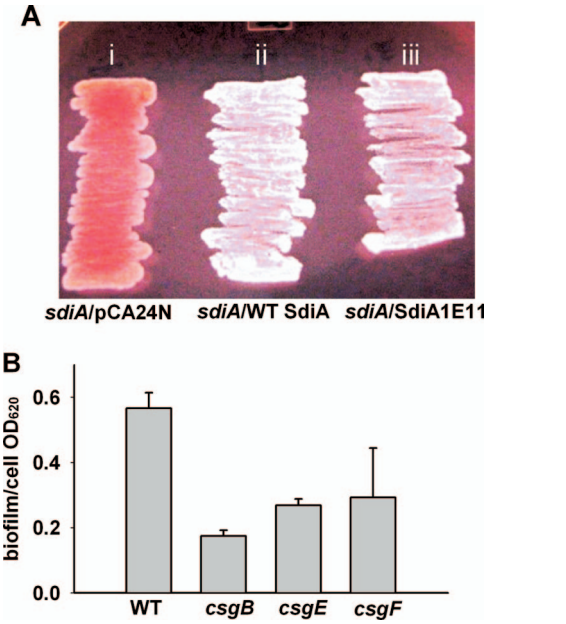

FIG. 4. (A) Curli production of BW25113 *sdiA* cells expressing no SdiA (empty vector) (i), wild-type SdiA (ii), and SdiA1E11 (iii) on a Congo red plate after 28 h in LB medium at 30°C. (B) Biofilm formation of BW25113 (WT), BW25113 *csgB*, BW25113 *csgE*, and BW25113 *csgF* in LB medium at 30°C after 24 h.

Evolved SdiA variants alter indole production. Since the whole-transcriptome and RT-PCR analyses showed that the most differentially expressed genes due to the mutations of variant SdiA1E11 versus wild-type SdiA were indole-related genes that were induced (*tnaAB* and *tnaC*) (Table 3), extracellular indole concentrations were measured with the SdiA variants. Corroborating the microarray data (induction of indole-producing *tnaA*), SdiA1E11 produced 9-fold more extracellular indole than wild-type SdiA at the same cell turbidity of 3 at 600 nm (Fig. 5), and SdiA1E11 also produced 9.6-fold more intracellular indole than wild-type SdiA (3.2 ± 0.5 versus 0.33 ± 0.09 nmol/mg total protein). Note that the chromosomal deletion of *sdiA* (*sdiA*/pCA24N versus BW25113/pCA24N) did not change indole production (Fig. 5). In con-

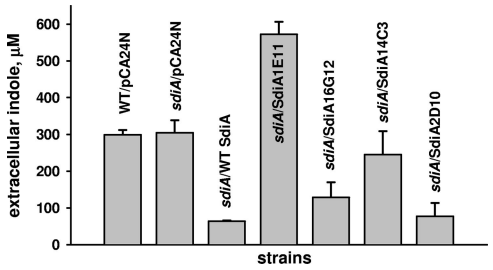

FIG. 5. Production of extracellular indole by BW25113 *sdiA* cells expressing the SdiA variants at a cell density of 3.0. Each experiment was repeated at least two times, and one standard deviation is shown. SdiA was expressed using 1 mM IPTG.

trast, the overexpression of full-length SdiA (SdiA2D10 and wild-type SdiA) decreased (fivefold) indole production, which was expected since a previous microarray result indicated that the overexpression of SdiA repressed *tnaA* by fourfold (55) and our RT-PCR results indicated the same repression. Therefore, evolving SdiA to reduce biofilm formation via variant SdiA1E11 resulted in the induction of *tnaA* which leads to more indole, which has been shown by us to reduce biofilm formation with 11 *E. coli* strains (17, 31, 32, 34, 64).

Also, the whole-transcriptome analysis showed that wild-type SdiA repressed (5- to 14-fold) the AI-2 uptake gene operon (*lsrKRACDBFG*) and SdiA1E11 induced (3- to 4-fold) those genes compared to wild-type SdiA (Table 3). Hence, these results also support that SdiA is associated with multiple signals, AHLs, AI-2, and indole (34).

SdiA1E11 functions via indole as evidenced by cell density, motility, and biofilm formation with double mutants. Since the mutations of SdiA1E11 decreased biofilm formation dramatically (Fig. 2A and B) and increased indole concentrations dramatically (Fig. 5), we hypothesized that SdiA1E11 may function through indole. To test this hypothesis, cell density and motility were evaluated for SdiA1E11. Cell density was chosen since quorum-sensing signals allow bacteria to monitor their own population density to coordinate the expression of specific genes (20), conditioned medium with unknown extracellular signals influences the final cell density of *E. coli* (60), and indole prevents cell division (10). Also, motility was examined since it positively influences biofilm formation in *E. coli* (41, 59), and indole reduces both biofilm formation and motility in *E. coli* (32). In order to confirm that these two phenotypes are related to indole and SdiA, cell growth and motility were measured in the presence of indole.

As shown in Fig. 6A, both of the two most-distinctive biofilm inhibition mutants, SdiA1E11 and SdiA14C3, reached a different final cell density, while the deletion of *sdiA* itself did not significantly change cell density; the mutations of SdiA1E11 decreased cell density by 18 ± 4%, and SdiA14C3 increased cell density by 16 ± 5% (note that the specific growth rates were nearly unchanged [see Table S2A in the supplemental material]). These results indicate that the quorum-sensing regulator SdiA may be evolved to control cell density. Also, the growth curves and the final cell density of the other two biofilm mutants, SdiA16G12 and SdiA2D10, were similar to those of wild-type SdiA (data not shown). Indole is clearly linked to

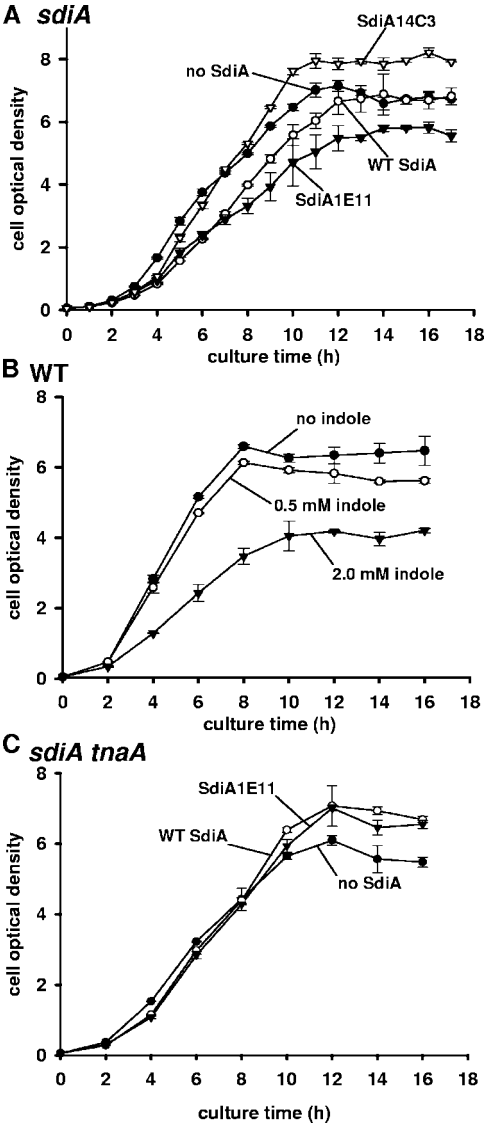

FIG. 6. Growth in LB medium at 30°C for BW25113 *sdiA* cells expressing the SdiA variants (A), BW25113 cells in the presence of indole (0, 0.5, and 2.0 mM) (B), and BW25113 *sdiA tnaA* cells expressing wild-type (WT) SdiA and SdiA1E11 (C). Each data point is the average of the results from at least two independent cultures. SdiA was expressed using 1 mM IPTG.

final cell density, as it decreases the cell density of the wild-type strain in a dose-dependent manner (Fig. 6B).

For cell motility, the overexpression of wild-type SdiA decreased (twofold) motility (*sdiA*/pCA24N versus *sdiA*/pCA24N-*sdiA* [Fig. 7A]), which is consistent with previous results (27), and the overexpression of wild-type SdiA completely complemented the *sdiA* deletion (*sdiA*/pCA24N-*sdiA* versus BW25113/pCA24N [Fig. 7A]). Also, the three low-biofilm-forming variants (SdiA1E11, SdiA16G12, and SdiA14C3) showed 1.5- to 1.7-fold less motility, which partially explains the biofilm reduction of these mutants. For SdiA1E11, motility was decreased, probably due to a high indole concentration (Fig. 5) since the addition of exogenous indole decreased motility in a dose-dependent manner (Fig. 7B).

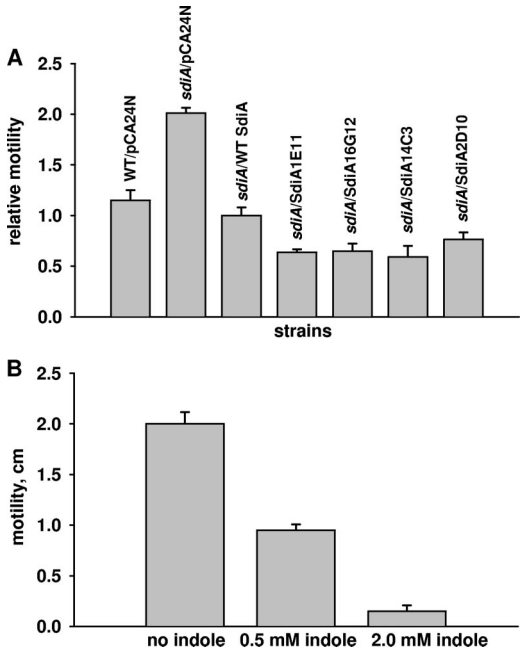

FIG. 7. Swimming motility of BW25113 *sdiA* cells expressing the SdiA variants (A) and BW25113 cells in the presence of indole (0, 0.5, and 2.0 mM) (B) after 20 h at 30°C. Each experiment was repeated two times, and one standard deviation is shown. SdiA was expressed using 1 mM IPTG.

Moreover, two double mutants, BW25113 *tnaA sdiA* and BW25113 *mtr sdiA* (Mtr is involved in indole import [61]) were constructed to investigate the effect of indole on biofilm formation with SdiA and SdiA1E11. As expected, BW25113 *tnaA sdiA* did not produce indole. In the *tnaA sdiA* strain, wild-type SdiA decreased biofilm formation compared to when no SdiA was expressed (Fig. 2C), as observed in the *sdiA* strain (Fig. 2B); however, SdiA1E11 increased rather than decreased biofilm formation unlike the results for wild-type SdiA (Fig. 2C). Also, with *tnaA sdiA*, SdiA1E11 did not appreciably decrease the final cell density compared to wild-type SdiA, while both wild-type SdiA and SdiA1E11 increased the final cell density compared to when no SdiA was expressed (Fig. 6C). Therefore, indole synthesis via *tnaA* is required for SdiA1E11 to alter cell phenotypes.

Mtr is less important for the mechanism of SdiA1E11; SdiA1E11 did not change biofilm formation compared to wild-type SdiA in the *mtr sdiA* mutant (not shown) but decreased the final cell density (not shown) as observed in the *sdiA* strain (Fig. 6A). For wild-type SdiA, both TnaA (Fig. 2C) and Mtr were not required for SdiA activity as SdiA decreased biofilm formation in the two double mutants. We also tried to construct double mutants of *sdiA luxS* and *sdiA lsrB* to investigate the mechanism of SdiA associated with AI-2 since SdiA most repressed AI-2 transport genes (Table 3). However, both double mutations were lethal, which shows the importance of SdiA and AI-2 and their interdependence.

Saturation mutagenesis and the truncation of SdiA. Since two SdiA variants (SdiA1E11 and SdiA2D10) have a truncation along with additional mutations at E31G, Y42F, and M94K (Fig. 1A) and since the amino acid residues of Y41 and W95 are highly conserved throughout the LuxR family (62), we investigated the importance of these and related positions of SdiA by substituting all possible amino acids via saturation mutagenesis using SdiA variants SdiA1E11 and SdiA2D10 as the parent proteins (saturation mutations at M94 and W95 for SdiA1E11 and saturation mutations at H28, E29, I30, E31, Y39, D40, Y41, and Y42 for SdiA2D10). After screening 1,762 colonies to ensure with a probability of 99% that all possible codons were utilized (47), we could not identify better variants that show a significant change in biofilm formation with and without 3o-C8-L-HSL than SdiA1E11 and SdiA2D10. For example, about 10% of the variants from the saturation mutagenesis at positions M94 and W95 of SdiA1E11 reduced biofilm formation similarly to the parent SdiA1E11.

Since three of the biofilm mutants (SdiA1E11, SdiA16G12, and SdiA14C3) contained truncations at the C terminus of SdiA (Fig. 1), we investigated the relationship between the length of SdiA and biofilm formation. Seven truncation mutants were constructed using site-directed mutagenesis to introduce a stop codon at R16, Q33, T53, A73, L93, A110, and L133 of SdiA. Four truncation variants (SdiAL133, SdiAA110, SdiAL93, and SdiAA73) lacking the carboxy-terminal DNA-binding domain of SdiA had a significant reduction in biofilm formation (3- to 10-fold) in both LB and LB glu media for 8 h (data not shown). Also, SdiAL133X decreased biofilm formation (10-fold) in LB glu medium compared to wild-type SdiA after 24 h, which is comparable with the 20-fold reduction in biofilm formation by SdiA1E11 having five mutations at F7L, F59L, Y70C, M94K, and K153X (Fig. 2B). Overall, these results confirm that the deletion of the C terminus of SdiA results in a reduction in biofilm formation.

DISCUSSION

Here we demonstrate that the quorum-sensing regulator SdiA may be evolved to control the biofilm formation of *E. coli*. Two main phenotypes were found: with SdiA1E11, biofilm formation is reduced an additional 20-fold, primarily due to increased indole concentrations, and with SdiA2D10, biofilm formation is increased 7-fold in the presence of C8-DL-HSL and 3o-C12-L-HSL. These results show that the cell's genetic circuitry may be rewired internally to both increase and decrease biofilm formation. Unlike where we controlled biofilm formation by manipulating indole extracellular concentrations by cloning a monooxygenase in a second bacterium (32), the current results are important for controlling biofilm formation with a single strain by controlling a sensor rather than the signal. Previous efforts to control biofilm formation by using synthetic circuits utilized the induction of *traA*, the conjugation plasmid pilin gene, upon exposure to UV light (29). Others have coordinated cell communication via quorum-sensing molecules and synthetic circuits but not controlled biofilm formation (7).

We determined that the mechanism by which SdiA1E11 reduces biofilm formation is through increased indole concentrations. The lines of evidence for this conclusion are that (i) the whole-transcriptome analysis shows *tnaA* is induced (Table 3), (ii) extracellular (Fig. 5) and intracellular indole concentrations were increased, (iii) motility is decreased (Fig. 7A) and indole addition to the host reduced motility in a dose-depen-

dent manner (Fig. 7B), (iv) cell density was decreased (Fig. 6A) and indole addition to the host reduced cell density in a dose-dependent manner (Fig. 6B), and (v) SdiA1E11 did not affect biofilm formation (Fig. 2C) or cell density in a *tnaA sdiA* double mutant (Fig. 6C).

Several physiological roles of SdiA have been determined along with the structure of the N-terminal AHL binding domain of SdiA (residues 1 to 171); however, the identification of the endogenous signal(s) from *E. coli* that binds to SdiA has been difficult. It is known that unidentified extracellular factors from conditioned medium are titrated by the N-terminal part of SdiA and prevent the induction of *E. coli* O157:H7 virulence factors (27), that the extracellular factors (even from AI-2-deficient strains) regulate the *ftsQ2p* cell division promoter via SdiA (21, 50), and that the extracellular factors decrease cell growth when the multidrug efflux pumps AcrAB are overexpressed (60); note that the overexpression of SdiA increases AcrAB expression (43). In all three cases, it is highly possible that indole is part of the unidentified extracellular component of the conditioned medium in these previous SdiA studies since it is abundant in the conditioned medium of stationary-phase cells (up to 600 μM in LB medium [17]) and since indole affects two of these phenotypes (indole decreases the *ftsQ2p* cell division promoter via SdiA [32]) and reduces cell growth (10, 32). Since some of these SdiA-mediated effects occur in $LuxS^-$ strains and since the synthesis of AI-2 and AI-3 depends on the presence of LuxS (51), AI-2 and AI-3 are unlikely to be the extracellular factors that interact with SdiA.

Additional evidence shows that indole and SdiA are related. Indole biofilm signaling requires SdiA (34), and indole signaling occurs primarily at 30°C (34) in a manner similar to SdiA responsiveness occurring mainly at 30°C but not at 37°C in *E. coli* (52). Both indole and SdiA decrease biofilm formation and motility (32), enhance antibiotic resistance (24, 34, 43), influence acid resistance (indole decreases and SdiA increases acid resistance) (32, 52), and regulate cell division (indole decreases and SdiA increases cell division) (10, 34, 54). In the current study, the mutation of SdiA significantly altered biofilm formation, cell density, indole production, and motility. However, how indole and SdiA are related and control cell physiology is unknown and should be investigated further since SdiA (like LasR and TraR [6]) is insoluble without AHLs binding it (62); yet, AHLs are not readily available (since *E. coli* does not produce them) and SdiA alters phenotypes in the absence of AHLs.

In this study, through the whole-transcriptome analysis (Table 3), we also found a new role for wild-type SdiA that explains its role in reducing early biofilm formation (Fig. 2A): SdiA decreases curli production via the repression of *csgDEFG* and *csgBAC* (Table 3). These DNA microarray results were corroborated with a curli assay (Fig. 4A). In addition, three curli *csgB*, *csgE*, and *csgF* mutants were used to show that the proteins encoded by these genes are directly related to biofilm formation (Fig. 4B). Curli fibers from *E. coli* show biochemical and biophysical properties of amyloid proteins that are associated with debilitating human ailments including Alzheimer's and prion diseases (11), and curli fibers function as a major structure of adherence that is essential for the biofilm formation of *E. coli* (42).

In contrast, we previously reported that in suspension cells, SdiA (the wild-type strain versus the *sdiA* deletion mutant) induces curli genes (*csgDEFG* and *csgBAC*) (34). Also, SdiA most represses genes involved in UMP biosynthesis (*carAB*, *pyrLBI*, *pyrF*, and *uraA*) in suspension cells (34), while in biofilm cells (this study), SdiA did not change the gene expression of these genes. Therefore, SdiA has distinctive roles for cells in suspension versus cells in biofilms.

In the current study, the truncation of the C-terminal DNA-binding domain of SdiA (K153X) and additional mutations (F7L, F59L, Y70C, and M94K) in SdiA1E11 dramatically increase indole production (Fig. 5) which leads to decreased biofilm formation (Fig.2AB) and decreased motility (Fig. 7), as indole decreases these two phenotypes (32). Notably three mutations (F59L, Y70C, and M94K) in SdiA1E11 are adjacent to the residues involved in the binding of *N*-octanoyl-homoserine lactones (Y63, W67, Y72, D80, and W95) (62), and three of the four mutations in SdiA1E11 (F7L, F59L, and Y70C) result in the loss of aromatic side chains. The truncation of the C terminus, which should abolish the DNA-binding activity of SdiA and retain the ligand-binding domain (62), enhances the control of SdiA over biofilm formation and should be investigated further. Since the overproduced N-terminal part of SdiA inhibits the expression of virulence factors in wild-type *E. coli* O157:H7 and negatively affects the activity of the full-length SdiA (27), it is interesting to investigate if truncated SdiA variants, such as SdiA1E11, alter the expression of virulence genes.

The overexpression of SdiA from a plasmid showed significant effects on cell division (54), increased mitomycin C resistance (56), and increased multidrug resistance (43), while the chromosomal deletion of *sdiA* had no effect or reduced effects on these phenotypes (43, 54, 56). We also observed that the overexpression of wild-type SdiA led to a significant decrease of *tnaA* expression (whole-transcriptome and RT-PCR results) along with reduced indole production (Fig. 5), while the chromosomal *sdiA* deletion did not affect indole production (Fig. 5), although the *sdiA* deletion itself significantly influenced biofilm formation, motility, and acid resistance (32). It was previously proposed that SdiA has very low levels of activity in pure culture (in the absence of AHLs) (2), that the overexpression of SdiA may override normal regulation (2), and that the overexpression of SdiA from a plasmid results in a large pleiotropic response (35). Most importantly, though, we were able to find SdiA mutations that allow us to increase or decrease biofilm formation, even if the role of SdiA remains incompletely characterized.

Natural bacterial biofilms are heterogeneous communities. Hence, many bacteria utilize quorum-sensing circuits to sense their own population density as well as to eavesdrop on quorum-sensing signals from other bacteria so that bacteria readily coordinate group behavior (such as biofilm formation and pathogenesis) in multispecies communities (8). Previously, it was suggested that both *Salmonella enterica* and *E. coli* utilize SdiA to eavesdrop on AHL from other strains (39) since the SdiA-regulated, outer membrane protein promoter *rckp* responded to several AHLs (*N*-butyryl- and *N*-oxobutyryl-, *N*-hexanoyl-, *N*-oxohexanoyl-, *N*-octanoyl-, *N*-oxooctanoyl-, *N*-decanoyl-, and *N*-oxodecanoyl-homoserine lactones). In the current study, an evolved SdiA variant (SdiA2D10) increased the biofilm formation of *E. coli* the most in the presence of

C8-DL-HSL and 3o-C12-L-HSL while wild-type SdiA decreased *E. coli* biofilm formation up to 51-fold in short-term experiments (32), and three AHL signals (*N*-butyryl-, *N*-hexanoyl-, and *N*-octanoyl-homoserine lactones) decreased biofilm formation with wild-type *E. coli* but not with the *sdiA* mutant (32). Therefore, we show here that *E. coli* can evolve SdiA to control biofilm formation in the presence of the signals of other microbial species. Similarly, indole and 7-hydroxyindole, which have been termed promiscuous biofilm signals (58), increase the biofilm formation of *P. aeruginosa* (which does not synthesize indole), decrease its production of virulence factors by repressing quorum-sensing related genes, and enhance multidrug resistance by inducing efflux pump genes (30). *P. aeruginosa* was also found to degrade indole and 7-hydroxyindole (30). Hence, *E. coli* may use indole to reduce the virulence of other bacteria, while other bacteria have acquired a defense system to cope with indole. Therefore, competition and adaptation are prevalent, and SdiA may play an important role in multispecies consortia.

Many bacteria contain more than one quorum-sensing circuit to adapt to diverse environmental conditions (8), and LuxR has been rapidly evolved for increased sensitivity to a broad range of AHLs (13). Similarly, *E. coli* has SdiA associated with multiple signals (e.g., indole, AHLs, and AI-2) (34). In this study, we demonstrate that the LuxR homolog SdiA may be readily evolved; as a result, evolved SdiA variants alter biofilm formation, cell density, indole concentration, and motility in *E. coli*. The mechanism of how pathogenic bacteria evolve such traits as antibiotic resistance within a short time is still unclear (1), and how strains interact with multiple species in natural biofilms is also unclear. This study implies that bacteria have the capability to evolve a quorum-sensing protein that is related to detecting other bacteria and that quorum-sensing proteins can be a target for biofilm control.

ACKNOWLEDGMENTS

This research was supported by the NIH (R01 EB003872) and ARO (W911NF-06-1-0408).

We thank the National Institute of Genetics (Japan) for providing the Keio and ASKA clones.

REFERENCES

1. **Aharoni, A., L. Gaidukov, O. Khersonsky, S. M. Gould, C. Roodveldt, and D. S. Tawfik.** 2005. The "evolvability" of promiscuous protein functions. Nat. Genet. **37:**73–76.
2. **Ahmer, B. M.** 2004. Cell-to-cell signalling in *Escherichia coli* and *Salmonella enterica*. Mol. Microbiol. **52:**933–945.
3. **Baba, T., T. Ara, M. Hasegawa, Y. Takai, Y. Okumura, M. Baba, K. A. Datsenko, M. Tomita, B. L. Wanner, and H. Mori.** 2006. Construction of *Escherichia coli* K-12 in-frame, single-gene knockout mutants: the Keio collection. Mol. Syst. Biol. **2:**2006.0008.
4. **Bansal, T., D. Englert, J. Lee, M. Hegde, T. K. Wood, and A. Jayaraman.** 2007. Differential effects of epinephrine, norepinephrine, and indole on *Escherichia coli* O157:H7 chemotaxis, colonization, and gene expression. Infect. Immun. **75:**4597–4607.
5. **Botsford, J. L., and R. D. DeMoss.** 1971. Catabolite repression of tryptophanase in *Escherichia coli*. J. Bacteriol. **105:**303–312.
6. **Bottomley, M. J., E. Muraglia, R. Bazzo, and A. Carfi.** 2007. Molecular insights into quorum sensing in the human pathogen *Pseudomonas aeruginosa* from the structure of the virulence regulator LasR bound to its autoinducer. J. Biol. Chem. **282:**13592–13600.
7. **Brenner, K., D. K. Karig, R. Weiss, and F. H. Arnold.** 2007. Engineered bidirectional communication mediates a consensus in a microbial biofilm consortium. Proc. Natl. Acad. Sci. USA **104:**17300–17304.
8. **Case, R. J., M. Labbate, and S. Kjelleberg.** 2008. AHL-driven quorum-sensing circuits: their frequency and function among the proteobacteria. ISME J. **2:**345–349.
9. **Chai, Y., and S. C. Winans.** 2004. Site-directed mutagenesis of a LuxR-type quorum-sensing transcription factor: alteration of autoinducer specificity. Mol. Microbiol. **51:**765–776.
10. **Chant, E. L., and D. K. Summers.** 2007. Indole signalling contributes to the stable maintenance of *Escherichia coli* multicopy plasmids. Mol. Microbiol. **63:**35–43.
11. **Chapman, M. R., L. S. Robinson, J. S. Pinkner, R. Roth, J. Heuser, M. Hammar, S. Normark, and S. J. Hultgren.** 2002. Role of *Escherichia coli* curli operons in directing amyloid fiber formation. Science **295:**851–855.
12. **Cherepanov, P. P., and W. Wackernagel.** 1995. Gene disruption in *Escherichia coli*: Tc^R and Km^R cassettes with the option of Flp-catalyzed excision of the antibiotic-resistance determinant. Gene **158:**9–14.
13. **Collins, C. H., F. H. Arnold, and J. R. Leadbetter.** 2005. Directed evolution of *Vibrio fischeri* LuxR for increased sensitivity to a broad spectrum of acyl-homoserine lactones. Mol. Microbiol. **55:**712–723.
14. **Collins, C. H., J. R. Leadbetter, and F. H. Arnold.** 2006. Dual selection enhances the signaling specificity of a variant of the quorum-sensing transcriptional activator LuxR. Nat. Biotechnol. **24:**708–712.
15. **Da Re, S., and J. M. Ghigo.** 2006. A CsgD-independent pathway for cellulose production and biofilm formation in *Escherichia coli*. J. Bacteriol. **188:**3073–3087.
16. **Davies, D. G., M. R. Parsek, J. P. Pearson, B. H. Iglewski, J. W. Costerton, and E. P. Greenberg.** 1998. The involvement of cell-to-cell signals in the development of a bacterial biofilm. Science **280:**295–298.
17. **Domka, J., J. Lee, and T. K. Wood.** 2006. YliH (BssR) and YceP (BssS) regulate *Escherichia coli* K-12 biofilm formation by influencing cell signaling. Appl. Environ. Microbiol. **72:**2449–2459.
18. **Edgar, R., M. Domrachev, and A. E. Lash.** 2002. Gene Expression Omnibus: NCBI gene expression and hybridization array data repository. Nucleic Acids Res. **30:**207–210.
19. **Fishman, A., Y. Tao, W. E. Bentley, and T. K. Wood.** 2004. Protein engineering of toluene 4-monooxygenase of *Pseudomonas mendocina* KR1 for synthesizing 4-nitrocatechol from nitrobenzene. Biotechnol. Bioeng. **87:**779–790.
20. **Fuqua, W. C., S. C. Winans, and E. P. Greenberg.** 1994. Quorum sensing in bacteria: the LuxR-LuxI family of cell density-responsive transcriptional regulators. J. Bacteriol. **176:**269–275.
21. **García-Lara, J., L. H. Shang, and L. I. Rothfield.** 1996. An extracellular factor regulates expression of *sdiA*, a transcriptional activator of cell division genes in *Escherichia coli*. J. Bacteriol. **178:**2742–2748.
22. **González Barrios, A. F., R. Zuo, Y. Hashimoto, L. Yang, W. E. Bentley, and T. K. Wood.** 2006. Autoinducer 2 controls biofilm formation in *Escherichia coli* through a novel motility quorum-sensing regulator (MqsR, B3022). J. Bacteriol. **188:**305–316.
23. **Henikoff, S., J. C. Wallace, and J. P. Brown.** 1990. Finding protein similarities with nucleotide sequence databases. Methods Enzymol. **183:**111–132.
24. **Hirakawa, H., Y. Inazumi, T. Masaki, T. Hirata, and A. Yamaguchi.** 2005. Indole induces the expression of multidrug exporter genes in *Escherichia coli*. Mol. Microbiol. **55:**1113–1126.
25. **Jayaraman, A., F. B. Mansfeld, and T. K. Wood.** 1999. Inhibiting sulfate-reducing bacteria in biofilms by expressing the antimicrobial peptides indolicidin and bactenecin. J. Ind. Microbiol. Biotechnol. **22:**167–175.
26. **Jayaraman, A., and T. K. Wood.** 2008. Bacterial quorum sensing: signals, circuits, and implications for biofilms and disease. Annu. Rev. Biomed. Eng. **10:**145–167.
27. **Kanamaru, K., K. Kanamaru, I. Tatsuno, T. Tobe, and C. Sasakawa.** 2000. SdiA, an *Escherichia coli* homologue of quorum-sensing regulators, controls the expression of virulence factors in enterohaemorrhagic *Escherichia coli* O157:H7. Mol. Microbiol. **38:**805–816.
28. **Kitagawa, M., T. Ara, M. Arifuzzaman, T. Ioka-Nakamichi, E. Inamoto, H. Toyonaga, and H. Mori.** 2005. Complete set of ORF clones of *Escherichia coli* ASKA library (a complete set of *E. coli* K-12 ORF archive): unique resources for biological research. DNA Res. **12:**291–299.
29. **Kobayashi, H., M. Kaern, M. Araki, K. Chung, T. S. Gardner, C. R. Cantor, and J. J. Collins.** 2004. Programmable cells: interfacing natural and engineered gene networks. Proc. Natl. Acad. Sci. USA **101:**8414–8419.
30. **Lee, J., C. Attila, S. L. G. Cirillo, J. D. Cirillo, and T. K. Wood.** 2009. Indole and 7-hydroxyindole diminish *Pseudomonas aeruginosa* virulence. Microb. Biotechol. **2:**75–90.
31. **Lee, J., T. Bansal, A. Jayaraman, W. E. Bentley, and T. K. Wood.** 2007. Enterohemorrhagic *Escherichia coli* biofilms are inhibited by 7-hydroxyindole and stimulated by isatin. Appl. Environ. Microbiol. **73:**4100–4109.
32. **Lee, J., A. Jayaraman, and T. K. Wood.** 2007. Indole is an inter-species biofilm signal mediated by SdiA. BMC Microbiol. **7:**42.
33. **Lee, J., R. Page, R. García-Contreras, J. M. Palermino, X. S. Zhang, O. Doshi, T. K. Wood, and W. Peti.** 2007. Structure and function of the *Escherichia coli* protein YmgB: a protein critical for biofilm formation and acid-resistance. J. Mol. Biol. **373:**11–26.
34. **Lee, J., X. S. Zhang, M. Hegde, W. E. Bentley, A. Jayaraman, and T. K. Wood.** 2008. Indole cell signaling occurs primarily at low temperatures in *Escherichia coli*. ISME J. **2:**1007–1023.

35. **Lindsay, A., and B. M. Ahmer.** 2005. Effect of *sdiA* on biosensors of *N*-acylhomoserine lactones. J. Bacteriol. **187:**5054–5058.
36. **Luján, A. M., A. J. Moyano, I. Segura, C. E. Argarana, and A. M. Smania.** 2007. Quorum-sensing-deficient (*lasR*) mutants emerge at high frequency from a *Pseudomonas aeruginosa mutS* strain. Microbiology **153:**225–237.
37. **Luo, Z.-Q., A. J. Smyth, P. Gao, Y. Qin, and S. K. Farrand.** 2003. Mutational analysis of TraR. Correlating function with molecular structure of a quorum-sensing transcriptional activator. J. Biol. Chem. **278:**13173–13182.
38. **Maeda, T., V. Sanchez-Torres, and T. K. Wood.** 2008. Metabolic engineering to enhance bacterial hydrogen production. Microb. Biotechnol. **1:**30–39.
39. **Michael, B., J. N. Smith, S. Swift, F. Heffron, and B. M. Ahmer.** 2001. SdiA of *Salmonella enterica* is a LuxR homolog that detects mixed microbial communities. J. Bacteriol. **183:**5733–5742.
40. **Moons, P., R. Van Houdt, A. Aertsen, K. Vanoirbeek, Y. Engelborghs, and C. W. Michiels.** 2006. Role of quorum sensing and antimicrobial component production by *Serratia plymuthica* in formation of biofilms, including mixed biofilms with *Escherichia coli*. Appl. Environ. Microbiol. **72:**7294–7300.
41. **Pratt, L. A., and R. Kolter.** 1998. Genetic analysis of *Escherichia coli* biofilm formation: roles of flagella, motility, chemotaxis and type I pili. Mol. Microbiol. **30:**285–293.
42. **Prigent-Combaret, C., G. Prensier, T. T. Le Thi, O. Vidal, P. Lejeune, and C. Dorel.** 2000. Developmental pathway for biofilm formation in curli-producing *Escherichia coli* strains: role of flagella, curli and colanic acid. Environ. Microbiol. **2:**450–464.
43. **Rahmati, S., S. Yang, A. L. Davidson, and E. L. Zechiedrich.** 2002. Control of the AcrAB multidrug efflux pump by quorum-sensing regulator SdiA. Mol. Microbiol. **43:**677–685.
44. **Reisner, A., K. A. Krogfelt, B. M. Klein, E. L. Zechner, and S. Molin.** 2006. In vitro biofilm formation of commensal and pathogenic *Escherichia coli* strains: impact of environmental and genetic factors. J. Bacteriol. **188:**3572–3581.
45. **Ren, D., L. A. Bedzyk, S. M. Thomas, R. W. Ye, and T. K. Wood.** 2004. Gene expression in *Escherichia coli* biofilms. Appl. Microbiol. Biotechnol. **64:**515–524.
46. **Ren, D., L. A. Bedzyk, R. W. Ye, S. M. Thomas, and T. K. Wood.** 2004. Differential gene expression shows natural brominated furanones interfere with the autoinducer-2 bacterial signaling system of *Escherichia coli*. Biotechnol. Bioeng. **88:**630–642.
47. **Rui, L., Y. M. Kwon, A. Fishman, K. F. Reardon, and T. K. Wood.** 2004. Saturation mutagenesis of toluene *ortho*-monooxygenase of *Burkholderia cepacia* G4 for enhanced 1-naphthol synthesis and chloroform degradation. Appl. Environ. Microbiol. **70:**3246–3252.
48. **Sambrook, J., E. F. Fritsch, and T. Maniatis.** 1989. Molecular cloning: a laboratory manual, 2nd ed. Cold Spring Harbor Laboratory Press, Cold Spring Harbor, NY.
49. **Schwede, T., J. Kopp, N. Guex, and M. C. Peitsch.** 2003. SWISS-MODEL: an automated protein homology-modeling server. Nucleic Acids Res. **31:**3381–3385.
50. **Sitnikov, D. M., J. B. Schineller, and T. O. Baldwin.** 1996. Control of cell division in *Escherichia coli*: regulation of transcription of *ftsQA* involves both *rpoS* and SdiA-mediated autoinduction. Proc. Natl. Acad. Sci. USA **93:**336–341.
51. **Sperandio, V., A. G. Torres, B. Jarvis, J. P. Nataro, and J. B. Kaper.** 2003. Bacteria-host communication: the language of hormones. Proc. Natl. Acad. Sci. USA **100:**8951–8956.
52. **Van Houdt, R., A. Aertsen, P. Moons, K. Vanoirbeek, and C. W. Michiels.** 2006. *N*-Acyl-*L*-homoserine lactone signal interception by *Escherichia coli*. FEMS Microbiol. Lett. **256:**83–89.
53. **Wang, D., X. Ding, and P. N. Rather.** 2001. Indole can act as an extracellular signal in *Escherichia coli*. J. Bacteriol. **183:**4210–4216.
54. **Wang, X. D., P. A. de Boer, and L. I. Rothfield.** 1991. A factor that positively regulates cell division by activating transcription of the major cluster of essential cell division genes of *Escherichia coli*. EMBO J. **10:**3363–3372.
55. **Wei, Y., J. M. Lee, D. R. Smulski, and R. A. LaRossa.** 2001. Global impact of *sdiA* amplification revealed by comprehensive gene expression profiling of *Escherichia coli*. J. Bacteriol. **183:**2265–2272.
56. **Wei, Y., A. C. Vollmer, and R. A. LaRossa.** 2001. In vivo titration of mitomycin C action by four *Escherichia coli* genomic regions on multicopy plasmids. J. Bacteriol. **183:**2259–2264.
57. **Winson, M. K., M. Camara, A. Latifi, M. Foglino, S. R. Chhabra, M. Daykin, M. Bally, V. Chapon, G. P. Salmond, B. W. Bycroft, et al.** 1995. Multiple *N*-acyl-*L*-homoserine lactone signal molecules regulate production of virulence determinants and secondary metabolites in *Pseudomonas aeruginosa*. Proc. Natl. Acad. Sci. USA **92:**9427–9431.
58. **Wood, T. K.** 2009. Insights on *Escherichia coli* biofilm formation and inhibition from whole-transcriptome profiling. Environ. Microbiol. **11:**1–15.
59. **Wood, T. K., A. F. González Barrios, M. Herzberg, and J. Lee.** 2006. Motility influences biofilm architecture in *Escherichia coli*. Appl. Microbiol. Biotechnol. **72:**361–367.
60. **Yang, S., C. R. Lopez, and E. L. Zechiedrich.** 2006. Quorum sensing and multidrug transporters in *Escherichia coli*. Proc. Natl. Acad. Sci. USA **103:**2386–2391.
61. **Yanofsky, C., V. Horn, and P. Gollnick.** 1991. Physiological studies of tryptophan transport and tryptophanase operon induction in *Escherichia coli*. J. Bacteriol. **173:**6009–6017.
62. **Yao, Y., M. A. Martinez-Yamout, T. J. Dickerson, A. P. Brogan, P. E. Wright, and H. J. Dyson.** 2006. Structure of the *Escherichia coli* quorum sensing protein SdiA: activation of the folding switch by acyl homoserine lactones. J. Mol. Biol. **355:**262–273.
63. **Yao, Y., M. A. Martinez-Yamout, and H. J. Dyson.** 2005. Backbone and side chain ^{1}H, ^{13}C and ^{15}N assignments for *Escherichia coli* SdiA1-171, the autoinducer-binding domain of a quorum sensing protein. J. Biomol. NMR **31:**373–374.
64. **Zhang, X. S., R. García-Contreras, and T. K. Wood.** 2007. YcfR (BhsA) influences *Escherichia coli* biofilm formation through stress response and surface hydrophobicity. J. Bacteriol. **189:**3051–3062.